MULTIPACTOR DISCHARGE ON A DIELECTRIC

R. A. Kishek and Y. Y. Lau, Department of Nuclear Engineering and Radiological Sciences,
University of Michigan, Ann Arbor, MI 48109-2104

Abstract

This paper proposes a novel theory of a single-surface multipactor discharge on a dielectric, such as an rf window. Using a Monte Carlo simulation, we obtain the susceptibility diagram, applicable to a wide range of materials, in terms of the rf electric field and of the DC electric field that may result from dielectric charging. The electron multiplication mechanism assumes realistic yield curves of secondary electrons, including distributions of emission velocities and angles for these electrons. The susceptibility diagram thus constructed allows an immediate assessment of the range of rf power over which multipactor may be expected to occur. A simple analytic theory which corroborates the simulation results is presented.

Multipactor discharge is an ubiquitous phenomenon observed in a multitude of devices that employ microwaves [1]. In the worst scenario, its presence leads to destruction of ceramic rf windows [1-2], erosion of metallic structures, melting of internal components, and perforation of vacuum walls [1]. Multipactor may occur when a metallic gap or a dielectric surface is exposed to an AC electric field under some favorable conditions, and its avoidance has been a major concern among workers on high power microwave sources, rf accelerators, and space-based communication systems [3].

In this paper, we present a theory of single-surface multipactor discharge on a dielectric, significantly extending the only existing theoretical treatment [2] on this subject known to us. We shall evaluate the combined action of an rf electric field that is parallel to the dielectric surface, and of a DC electric field normal to the surface that is assumed to be present as a result of dielectric charging. This surface charging has been experimentally verified, with the resulting electric field measured to be as high as 4 kV/cm [1-2]. We shall compute the multipactor growth, using realistic yield curves of secondary electron emission. A Monte Carlo simulation is performed to account for the distributions of the emission velocities and emission angles of the secondary electrons. We ignore the space charge effects, rf loading by the multipactor, and the saturation mechanism (if any).

The geometry for this type of single-surface multipactor is shown in Fig. 1. Electrons emitted with a random velocity, v_o, and a random angle, ϕ, with respect to the positive y-axis, are subjected to forces imposed by the electric fields. The rf electric field, of magnitude E_{rfo} and frequency ω, acts only in the y-direction and imparts energy to the multipactor electrons, as well as translates them along the y-axis. The DC electric field, E_{DC}, does not impart any energy to the electrons. An electron emitted from the surface with a non-zero emission velocity is bent back by the restoring DC electric field and strikes the surface at a later time. During its transit, the electron gains energy only from the rf electric field, in a direction parallel to the surface. Thus upon impact, the electron strikes with much larger energy, and therefore emits a number of secondary electrons. This process repeats and, eventually, a large amount of energy gained from the rf electric field will be deposited on the surface, possibly leading to surface damage or breakdown.

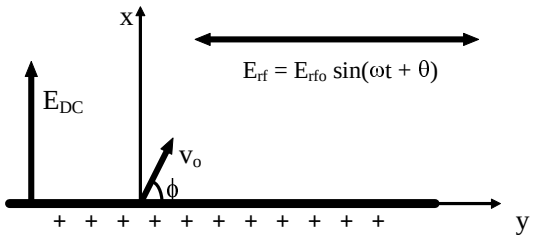

Fig. 1 Model of a single-surface multipactor in a parallel rf and normal DC electric fields.

The secondary electron yield, δ, is a function of the impact energy of the primary electron, E_i, and the angle to the normal, ξ, at which it strikes the surface. For the dependence of yield on impact energy, we will adopt Vaughan's empirical formula [4] which is characterized by two material-dependent parameters: the maximum yield, δ_{max}, and the energy at which it occurs, E_{max}. Two values of impact energy, termed the first and second crossover points, E_1 and E_2 respectively, result in a yield of 1, while $\delta > 1$ in between.

For impact at an angle, the parameters E_{max} and δ_{max} are adjusted in calculating the yield, according to the following equations [4]:

$$\begin{aligned} E_{max} &= E_{max0}\left(1+\frac{k_s\xi^2}{\pi}\right) \\ \delta_{max} &= \delta_{max0}\left(1+\frac{k_s\xi^2}{2\pi}\right) \end{aligned} \quad . \qquad \textbf{(1)}$$

Here E_{max0} and δ_{max0} are the parameters for an impact angle of 0° (i.e. normal to the surface), and k_s is a surface smoothness factor ranging from 0 for a rough surface to 2 for a polished surface. In this paper we set $k_s = 1$, representing a typical dull surface [4]. It is worth noting that in this situation, since the electrons gain their energy from the parallel rf, most impacts will be at almost grazing incidence ($\xi = \pi/2$).

0-7803-4376-X/98/$10.00 © 1998 IEEE

In the following analysis we shall use the following normalization scales: $1/\omega$ for time, E_{max0} for energies, $u = \sqrt{E_{max0}/m}$ for velocities, and $F = (\omega/e)\sqrt{mE_{max0}}$ for electric fields, where e = 1.602 × 4^{-19} C and m is the electron mass. Consider an electron launched at t = 0 from the surface at y = 0. It experiences a force due to the rf electric field, $E_{rfo}\sin(\omega t + \theta)$, which has a phase θ at the time of launch. The emission velocity, v_o, and angle from positive y-axis, φ, are assumed to be random. Solving the equations of motion for the electron gives an expression for the impact energy:

$$E_{ix} = \tfrac{1}{2} v_o^2 \sin^2\phi$$

$$E_{iy} = \frac{E_{rfo}^2}{2}\left[\cos\left(\frac{2v_o\sin\phi}{E_{DC}} + \theta\right) - \cos(\theta) + \frac{v_o\cos\phi}{E_{rfo}}\right]^2, \quad \textbf{(2)}$$

where E_{ix} and E_{iy} are the x and y components, respectively, of the impact energy. The impact angle is then:

$$\xi = \arctan\left(\sqrt{\frac{E_{iy}}{E_{ix}}}\right). \quad \textbf{(3)}$$

Given the impact energy and angle, the yield is determined.

To estimate the growth rate of the multipactor discharge, we follow the trajectory of a weighted macroparticle over a large number of impacts in a Monte Carlo simulation. The initial rf phase, θ, is uniformly distributed over $0 < \theta < 2\pi$. Each time a macroparticle leaves the surface, we assign it a random initial energy $E_o = \tfrac{1}{2} v_o^2$ and angle φ, according to the following distributions:

$$f(E_o) = \frac{E_o}{E_{om}^2} e^{-E_o/E_{om}}, \quad \textbf{(4a)}$$

$$g(\phi) = \tfrac{1}{2}\sin\phi, \quad \textbf{(4b)}$$

where E_{om} is the peak of the distribution of emission energies [note that the expected value of E_o is $2E_{om}$, and that $\int g(\phi)d\phi = 1$ over $0 < \phi < \pi$].

Substituting the random values of initial energy (velocity) and angle into Eqs. (2) and (3), we obtain the impact energy and, hence, the secondary electron yield for that transit. We use this value of the yield to adjust the charge on the macroparticle, then emit it again with a random velocity. Observing the time evolution of the charge on the macroparticle over a sufficiently long time, we can see either an exponentially growing or an exponentially decaying trend, depending on the external parameters chosen (E_{DC}, E_{rfo}, and δ_{max0}. A growth rate of zero identifies a point on the boundary of the multipactor region.

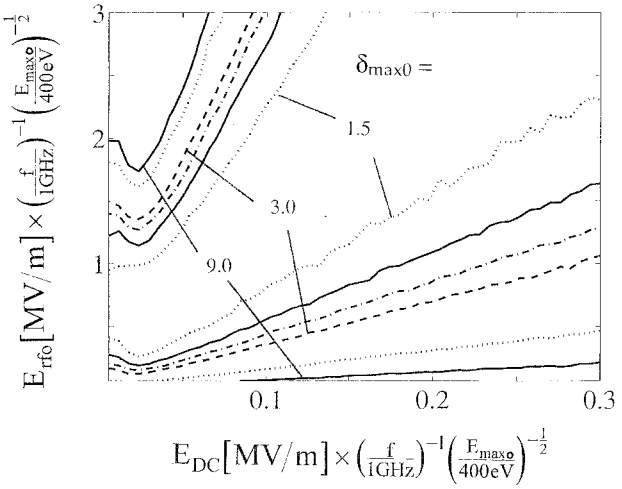

Fig. 2 Composite plot of multipactor region boundaries in the plane of (E_{DC}, E_{rfo}) for various values of δ_{max0} [from the innermost boundaries, δ_{max0} = 1.5, 2.0, 2.5, 3.0, 6.0, and 9.0], assuming E_{om}/E_{max0} = 0.005.

Figure 2 shows the boundary regions for selected values of δ_{max0}, corresponding to typical materials used in rf windows [see Table 1]. This susceptibility curve can be quite useful. A glance at Figure 2 indicates the range of rf power over which the window may be subject to multipactor. If the design parameters lie within the multipactor boundaries (positive growth rate) then multipactor is possible and the design needs to be modified. This can be done, for example, by changing the rf level, or by adding a slightly conductive coating to the window to reduce the static charge accumulation and the resulting DC field. Alternatively, the window may be coated with a material having low δ_{max0} (e.g., TiN). These measures have been employed in practice [1-2], although perhaps not systematically but rather by trial and error.

Table 1 Typical secondary electron emission parameters for materials commonly used in rf windows [adapted from ref. 5].

Material	δ_{max0}	E_{max0} (eV)	E_1/E_{max0} (grazing incidence)	E_2/E_{max0}
Al_2O_3 (alumina)	1.5-9	350-1300	0.23-0.011	10.2-24.5
Quartz-glass	2.9	420	0.072	15.6
Pyrex	2.3	340-400	0.107	13.7
Technical glasses	2-3	300-420	0.136-0.068	12.6-15.9
SiO_2 (quartz)	2.4	400	0.099	14.1

Following is the physical explanation for the shape of the susceptibility curves [Fig. 2]. For any given values of the fields, the growth rate is determined by the average value of the secondary electron yield, averaged over the random emission energy and angle distributions [Eqs. (4a) and (4b)]. Changing the magnitude of the rf

electric field changes the amount of energy the electron gains. Changing the DC field changes the amount of time spent in flight, and hence also the amount of energy gained. Since the secondary electron yield is above unity only for impact energies in between the two crossover points, if the rf electric field is too high or too low, then the amount of energy gained will vary accordingly, and thus the impact energy will fall outside of this region, where $\delta < 1$. This explains the existence of upper and lower boundaries. Now if the DC field is increased, the electron spends less time in flight, and so the rf electric field must be increased to maintain the same impact energy and yield. Preist and Talcott mention experimental evidence for the existence of the lower bound (E_{rfmin}) and predict the existence of an upper bound (E_{rfmax}) [2].

The preceding physical understanding of the phenomenon is useful in constructing an analytic solution for the susceptibility curve boundaries. First, we assume that all electrons are emitted normal to the surface, with an energy equal to the average energy of the emission energy distribution ($E_o = 2\,E_{om}$). As will be seen, this assumption does not qualitatively change the solution. Hence, substituting $E_o = 2\,E_{om}$ and $\phi = 90°$ into Eq. (2), averaging over θ, and setting the resulting average impact energy equal to E_1, then E_2, we obtain the following equations for the lower and upper boundaries, respectively:

$$E_{rf\,min} = \sqrt{\frac{2E_1}{1-\cos\left(4\sqrt{E_{om}}/E_{DC}\right)}} \qquad \textbf{(5a)}$$

$$E_{rf\,max} = \sqrt{\frac{2E_2}{1-\cos\left(4\sqrt{E_{om}}/E_{DC}\right)}} \qquad \textbf{(5b)}$$

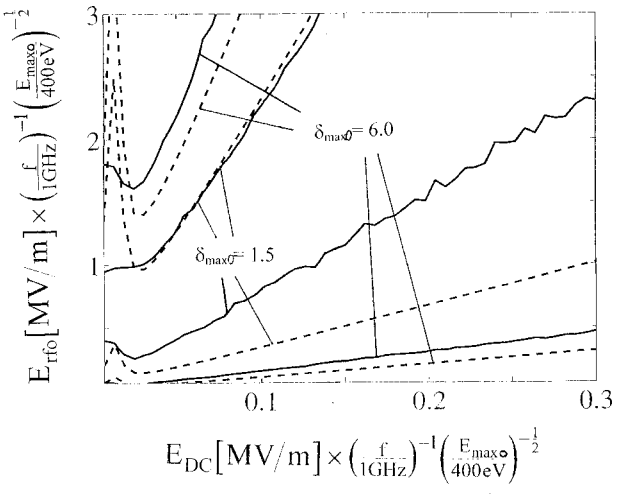

Fig. 3 Multipactor regions derived analytically (dashed) compared with ones obtained through Monte Carlo simulations (solid) for $\delta_{max0} = 1.5$ and $\delta_{max0} = 6.0$. Here, $E_{om} / E_{max0} = 0.005$.

These boundaries are compared in Figure 3 to the ones obtained from Monte Carlo simulations. We assume $E_{om} = 0.005$. As can be seen, the agreement is reasonably good, considering all the approximations involved. The slopes of the curves in Fig. 3, in the limit of large E_{DC}, are $\frac{1}{2}\sqrt{E_{1,2}/E_{om}}$, as easily deduced from Eqs. (5a) and (5b). Since impact is close to grazing, $\xi = \pi/2$, the values of E_1 and E_2 for grazing incidence should be used in Eqs. (5a) and (5b) [these values are listed for some materials in Table 1].

Finally, we note some differences between multipactor on a dielectric and on a metal surface. Since the impact angles of multipactor electrons on a dielectric are close to the grazing angle, the secondary electron yield would always be higher than that on a metal surface. In the steady state, multipactor on a metal surface has a secondary yield hovering around unity at the first cross-over point E_1 [3]. Our simulations so far cannot predict whether multipactor on a dielectric would saturate, but they seem to indicate that as the multipactor grows, the impact energies tend to prefer E_{max}, at which δ is maximum. Moreover, single-surface multipactor on a dielectric is less sensitive to the resonance condition that characterizes the 2-surface multipactor; it can therefore occur over a wider range of rf electric fields and phases. All of these, together with the poor heat conduction on a dielectric, perhaps partially explain the well-known vulnerability of ceramic windows to rf breakdown.

We wish to acknowledge Professor Ronald Gilgenbach and Agust Valfels for many valuable discussions. We also wish to thank Amadi Nwakanpa and Ghassan Shahin for computational support. This work was supported by the Multidisciplinary University Research Initiative (MURI), managed by the Air Force Office of Scientific Research and subcontracted through Texas Tech University, by the Department of Navy Grant N00014-97-1-G001 issued by the Naval Research Laboratory, and by the Northrop Grumman Industrial Affiliates Program.

REFERENCES

[1] J. R. M. Vaughan, IEEE Trans. **ED-8**, 302 (1961); **ED-15**, 883 (1968); **ED-35,** 1172 (1988).

[2] D. H. Preist and R. C. Talcott, IRE Trans. **ED-8**, 243 (1961).

[3] R. A. Kishek, Y. Y. Lau, and D. Chernin, Phys. Plasmas, **4**, 863 (1997); R. A. Kishek, Ph.D. Thesis, University of Michigan, Ann Arbor (1997).

[4] J. R. M. Vaughan, IEEE Trans. **ED-36**, 1963 (1989).

[5] O. Hachenberg and W. Brauer, "Secondary Electron Emission from Solids", A*dvances in Electronics and Electron Physics* **XI**, 413-499 (1959).